

Lyapunov-Based Reinforcement Learning State Estimator

Liang Hu¹, Chengwei Wu², and Wei Pan³

Abstract—In this paper, we consider the state estimation problem for nonlinear discrete-time stochastic systems. We combine Lyapunov’s method in control theory and deep reinforcement learning to design the state estimator. We theoretically prove the convergence of the bounded estimate error solely using the data simulated from the model. An actor-critic reinforcement learning algorithm is proposed to learn the state estimator approximated by a deep neural network. The convergence of the algorithm is analysed. The proposed Lyapunov-based reinforcement learning state estimator is compared with a number of existing nonlinear filtering methods through Monte Carlo simulations, showing its advantage in estimating convergence even under some system uncertainties such as covariance shift in system noise and randomly missing measurements. This is the first reinforcement learning-based nonlinear state estimator with bounded estimate error performance guarantee to the best of our knowledge.

Index Terms—Nonlinear filtering, deep reinforcement learning, Lyapunov stability.

I. INTRODUCTION

State estimation, inferring unknown states using noisy measurements and underlying model of the dynamic system, has found its important application in different areas ranging from control engineering, robotics, tracking and navigation to machine learning [1]–[4]. For linear stochastic systems with Gaussian noise, the renowned Kalman filter [5] is proved to give the optimal estimate with elegant convergence properties in estimate error covariance. For nonlinear stochastic systems, since the probability distribution of the state does not preserve the property of Gaussian, a closed-form estimator like Kalman filter generally does not exist. As a result, many nonlinear state estimation methods based on different approximation techniques have been proposed, among which the extended Kalman filter (EKF), unscented Kalman filter (UKF) [6] and particle filter (PF) [7] have been most widely used. For nonlinear systems with Gaussian noise, the EKF and UKF approximate the system state by a Gaussian distribution using the linearisation technique and the deterministic sampling method. For nonlinear non-Gaussian systems, the PF uses sequential Monte Carlo methods to approximate distribution of the state by a finite number of particles.

A fundamental problem of state estimation is how to design a state estimator such that the estimation error can be guaranteed to be bounded. This problem is challenging and scarcely addressed only in certain scenarios under some assumptions

[8]–[10]. In [8], it is proved that if the linearisation error is negligible, the local asymptotic stability of the EKF can be ensured. In [9], the estimate error of the discrete-time EKF remains bounded only if the initial estimate error is sufficiently small and system noise intensity is small. In [10], similar results can also be found for the UKF. Nonetheless, it is hard to reduce the initial estimate errors and linearisation errors in the deployment of the EKF and UKF, making these convergence conditions less applicable. For the PF, though it is theoretically proved that the estimate performance converges asymptotically to the optimal estimates as the number of particles goes to infinity in [11], only a limited particle can be used in practice due to the expensive online computation as the number of particle increases. Unfortunately, there are not any guarantees on estimation performance for the PF with limited particles. By summarising the EKF, UKF and PF observations, it is expected that an ideal state estimator can estimate the state with bounded estimate error performance guarantee for nonlinear non-Gaussian systems. Moreover, the performance guarantee should not rely on conditions of the initial estimate error, the system noise level, or the degree of nonlinearity of the underlying dynamic system. In this paper, we are interested in seeking a reinforcement learning (RL) based method to design such a state estimator.

RL was first applied to the state estimation problem in [12], where impressive estimation performance was shown. However, the theoretical guarantee on the convergence of bounded estimate error was unavailable, thus making it less applicable for practical applications [13]. More recently, an RL based Kalman filter design method was proposed in [14], in which the bounded estimate error can be guaranteed by using finite samples for stable linear systems. Another closely related research is (deep) neural network based state estimation [15]–[17] where neural networks are used to learn system models. Recurrent neural networks (RNNs) for state estimation has been explored in [15], [16], and DNNs has been introduced for Kalman filtering in [17]. Inspired by these works, we will combine deep learning and reinforcement learning, a.k.a., deep reinforcement learning (DRL), to design a state estimator in which the filter gain function will be learned using a deep neural network (DNN) from the sequence of estimate errors. Once the estimator is trained well offline, it can be deployed online and supposed to be efficient given the advance in DNN microprocessor for online applications. The key questions are how to prove the bounded estimate error guarantee in an RL setup and design an efficient learning algorithm with such a guarantee.

Motivated by [8]–[10], we plan to prove the stability of the estimate error dynamics; after that, the bounded estimate error can be guaranteed. In particular, we make no assumptions

¹Liang Hu is with the School of Computer Science and Electronic Engineering, University of Essex, UK. Email: l.hu@essex.ac.uk.

²Chengwei Wu is with the School of Astronautics, Harbin Institute of Technology, China. He is also with the Department of Cognitive Robotics, Delft University of Technology, Netherlands. Email: c.wu-1@tudelft.nl.

³Wei Pan is with the Department of Cognitive Robotics, Delft University of Technology, Netherlands. Email: wei.pan@tudelft.nl.

typically used in these results, such as initial estimate error, linearisation errors or assumptions on model nonlinearities, etc. Similar to [12], the mathematical model can be seen as a simulator, and the training of estimator is solely from data simulated using the mathematical model. Unfortunately, the data-based stability analysis of closed-loop systems in a model-free RL manner is still an open problem [13], [18]. Typically, Lyapunov's method in control theory is widely used to analyse the stability of dynamical systems. In [19], the stability of a deterministic nonlinear system was analysed using Lyapunov's method, assuming that the discount of the infinite-horizon cost is sufficiently close to 1. However, such an assumption makes it difficult to guarantee the learned policy's optimality without introducing certain extra assumptions [20]–[22]. As a basic tool in control theory, the construction/learning of the Lyapunov function is not trivial [23], [24]. In [25], the RL agent controls the switch between designed controllers using Lyapunov domain knowledge so that any policy is safe and reliable. [26] proposes a straightforward approach to construct the Lyapunov functions for nonlinear systems using DNNs. In [27], [28], a learning-based approach for constructing Lyapunov neural networks to ensure stability was proposed based on the assumption that the learned model is a Gaussian process, Lipschitz continuous and on discretised points in the subset of low-dimensional state space. Only until recently, the asymptotic stability in model-free RL is given for robotic control tasks [29]. In [30], [31], the stability of a system with a combination of a classic baseline controller and an RL controller is proved for autonomous surface vehicles with collisions.

In summary, we will combine Lyapunov's method in control theory and deep reinforcement learning to design state estimators for nonlinear stochastic discrete-time systems with bounded estimate error guarantee. The theoretical result is obtained by solely using the data simulated from the model. In our method, the estimator is trained/learned offline and then deployed directly using a DNN. Moreover, our state estimator is shown to be robust to system uncertainties, i.e., unknown measurement noise, missing measurement and non-Gaussian noise, which makes our method more applicable. The main contribution of the paper has twofold:

- 1) For the first time, a deep reinforcement learning method has been employed for nonlinear state estimator design;
- 2) The bounded estimate error can be theoretically guaranteed by solely using data regardless of the degree of model nonlinearities and noise distribution.

This is the first reinforcement learning-based nonlinear state estimator design method with bounded estimate error guarantee to the best of our knowledge.

The rest of the paper is organised as follows. In Section II, the state estimation problem of nonlinear stochastic discrete-time systems is formulated. In Section III, the theoretical result on bounded estimate error guarantee is proved. In Section IV, the learning algorithm is derived and the algorithm convergence is analysed. In Section V, our method is compared with EKF, UKF and PF in simulations. Conclusion is given in Section VI.

Notation: The notation used here is fairly standard except where otherwise stated. \mathcal{Z}_+ denotes the set of non-negative

integrals. \mathbb{R}^n and $\mathbb{R}^{n \times m}$ denote, respectively, the n dimensional Euclidean space and the set of all $n \times m$ real matrices. A^\top represents the transpose of A , and $\mathbb{E}\{x\}$ stands for the expectation of the stochastic variable x . $x \sim \mathcal{N}(m, N)$ with $m \in \mathbb{R}^n$ and $N \in \mathbb{R}^{n \times n}$ denotes the probability function of the random variable x follows a Gaussian distribution with m and N as the expectation and covariance, respectively. $\|x\|$ denotes 2-norm of the vector x , i.e., $\|x\| = x^\top x$.

II. PROBLEM FORMULATION

In this paper, we consider the state estimation problem for the following nonlinear discrete-time stochastic systems:

$$\begin{aligned} x_{k+1} &= f(x_k) + w_k, \\ y_k &= g(x_k) + v_k, \end{aligned} \quad (1)$$

where $x_k \in \mathbb{R}^n$, $y_k \in \mathbb{R}^m$ are the state and measurement, respectively, and w_k and v_k are stationary stochastic noise. The nonlinear functions $f(\cdot)$ and $g(\cdot)$ and the probability distributions of process noise w_k and measurement noise v_k are assumed to be all known, and the noise may be non-Gaussian.

A. State estimation

To estimate the state of system (1), the state estimator is typically designed in the following form:

$$\hat{x}_{k+1} = f(\hat{x}_k) + a(\hat{x}_k)e_{k+1} \quad (2)$$

where \hat{x}_k is the estimate of state x_k , $a(\cdot)$ is a linear/nonlinear function that can be calculated using various approximation methods and the measurement prediction error is given as follows:

$$e_{k+1} = y_{k+1} - g(f(\hat{x}_k)) \quad (3)$$

The form of the state estimator in (2) is standard and widely used in some existing estimation algorithms, such as the Kalman filter (KF) and extended Kalman filter (EKF). In the EKF, the state estimator of (1) is given as follows:

$$\hat{x}_{k+1} = f(\hat{x}_k) + K_k e_{k+1} \quad (4)$$

where K_k is the estimator gain at time instant k that is calculated using partial derivatives of the f and g at \hat{x}_k . As a result, the estimator gain K_k is actually a function of \hat{x}_k . Similarly, in the unscented Kalman filter (UKF), $a(\hat{x}_k)$ in (2) is instantiated using deterministic sampling methods. As for the particle filter (PF), even though no estimator gain is used explicitly, the importance weights of particles could be viewed as the function of $a(\hat{x}_k)$ in the sampling form. In this paper, our high-level plan is to approximate $a(\cdot)$ as a generic nonlinear function, i.e., a deep neural network, which can be learned from estimate errors data $x_k - \hat{x}_k$ over time.

Remark 1. *This paper will focus on the state estimation problem while two other closely related problems need to be remarked, i.e., state prediction and smoothing. In the state-prediction, measurement up to the current time instant is used to predict the state in the future; in the state-smoothing, measurement up to the current time instant is used to interpolate the state in the past. Our method proposed can be easily adapted to state prediction and smoothing problems as well.*

Definition 1. [9] The estimate error $\tilde{x}_k \triangleq x_k - \hat{x}_k$ is said to be exponentially bounded in mean square if $\exists \eta > 0$ and $0 < \varphi < 1$, such that

$$\mathbb{E}[\|\tilde{x}_k\|^2] \leq \eta \mathbb{E}[\|\tilde{x}_0\|^2] \varphi^k + p, \quad (5)$$

holds at all the time instants $k \geq 0$, where p is a positive constant number.

In this paper, we aim to learn the state estimator policy function $a(\cdot)$ in the estimator (2) using deep reinforcement learning such that the estimate error of the estimator (2) is guaranteed to converge exponentially to a positive bound in the mean square, as defined in Definition 1. In the following, we will introduce the background on reinforcement learning and show how to analyse the stability using Lypapunov's method.

III. REINFORCEMENT LEARNING AND DATA-BASED LYAPUNOV STABILITY ANALYSIS

In this section, the filtering error dynamics is described as a Markov decision process. Then, some preliminaries of reinforcement learning are presented. Next, a theorem is proposed to prove the boundness of estimate error.

A. Markov Decision Process

The estimate error dynamics of the state estimator design (2) can be described by a Markov decision process (MDP), which is defined as a tuple $\langle \mathcal{S}, \mathcal{A}, \mathcal{P}, \mathcal{C}, \gamma \rangle$. Here, \mathcal{S} is the state space, \mathcal{A} is the action space, \mathcal{P} is the transition probability distribution, \mathcal{C} is the cost¹, and $\gamma \in [0, 1)$ is the discount factor. Then we have

$$\tilde{x}_{k+1} \sim \mathcal{P}(\tilde{x}_{k+1} | \tilde{x}_k, a_k), \forall k \in \mathbb{Z}_+, \quad (6)$$

where \tilde{x}_k and \mathcal{C}_k are the state and cost at time instant k and $\tilde{x}_k \in \mathcal{S}$. An action $a(\cdot)$ at the state $\tilde{x}(\cdot)$ is sampled from the policy $\pi(a(\cdot) | \tilde{x}(\cdot))$. The standard state estimator (2) is naturally a special case of (6).

B. Reinforcement learning

In this paper, the objective is to find an optimal policy to minimise the expected accumulated cost as a value function:

$$V_\pi(\tilde{x}_k) = \sum_k \sum_{a_k} \pi(a_k | \tilde{x}_k) \sum_{\tilde{x}_{k+1}} \mathcal{P}_{k+1|k}(\mathcal{C}_k + \gamma V_\pi(\tilde{x}_{k+1})), \quad (7)$$

where $\mathcal{P}_{k+1|k} = \mathcal{P}(\tilde{x}_{k+1} | \tilde{x}_k, a_k)$ is the transition probability of the estimate error \tilde{x}_k , $\mathcal{C}_k = \mathcal{C}(\tilde{x}_k, a_k)$ is the cost function where we are interested in the quadratic form $\mathcal{C}_k = \tilde{x}_k^\top \tilde{x}_k$ in this paper, $\gamma \in [0, 1)$ is a constant discount factor, and $\pi(a_k | \tilde{x}_k)$ is a policy to be learned. In RL, the policy (nonlinear filter gain function in this paper) $\pi(a_k | \tilde{x}_k)$ is typically a Gaussian distribution:

$$\pi(a | \tilde{x}) = \mathcal{N}(a(\tilde{x}), \sigma), \quad (8)$$

from which an action $a_k \in \mathcal{U}$ at the state $\tilde{x}_k \in \mathcal{S}$ is sampled [32]. During the inference, the mean value $a(\tilde{x})$ is applied.

¹We will use cost instead of reward in this paper which is often used in control literature. Maximisation in RL setup will be minimisation instead.

During the training process, a Q-function $Q_\pi(\tilde{x}_k, a_k)$ (i.e., the action-value function) is practically minimised. $Q_\pi(\tilde{x}_k, a_k)$ is given as

$$Q_\pi(\tilde{x}_k, a_k) = \mathcal{C}_k + \gamma \mathbb{E}_{\tilde{x}_{k+1}} [V_\pi(\tilde{x}_{k+1})], \quad (9)$$

where $\mathbb{E}_{\tilde{x}_{k+1}}[\cdot] = \sum_{\tilde{x}_{k+1}} \mathcal{P}_{k+1|k}[\cdot]$ is an expectation operator over the distribution of \tilde{x}_{k+1} .

Soft actor-critic (SAC) algorithm is one of the state-of-the-art off-policy actor-critic RL algorithms [33]. In SAC, an entropy item is added to the Q-function as a regulariser, with which the exploration performance becomes adjustable. Based on (9), the Q-function with the entropy item is described as

$$Q_\pi(\tilde{x}_k, a_k) = \mathcal{C}_k + \gamma \mathbb{E}_{\tilde{x}_{k+1}} [V_\pi(\tilde{x}_{k+1}) - \alpha \mathcal{H}(\pi(a_{k+1} | \tilde{x}_{k+1}))], \quad (10)$$

where $\mathcal{H}(\pi(a_k | \tilde{x}_k)) = -\sum_{a_k} \pi(a_k | \tilde{x}_k) \ln(\pi(a_k | \tilde{x}_k)) = -\mathbb{E}_\pi[\ln(\pi(a_k | \tilde{x}_k))]$ is the entropy of the policy, and α is a temperature parameter. It is defined to determine the relative importance of the entropy term [33].

Thus, the algorithm is to solve the following optimisation problem.

$$\pi^* = \arg \min_{\pi \in \Pi} (\mathcal{C}_k + \gamma \mathbb{E}_{\tilde{x}_{k+1}} [V_\pi(\tilde{x}_{k+1}) - \alpha \mathcal{H}(\pi(a_{k+1} | \tilde{x}_{k+1}))]), \quad (11)$$

where Π is the policy set.

An optimal policy $\pi^*(a | \tilde{x}) = \mathcal{N}(a^*(\tilde{x}), \sigma^*)$ can be obtained by solving (11). Here, σ^* is close to 0, which further implies the optimal policy a^* converges to a deterministic mean value. Once such a policy is obtained, it can be deployed to the target system. For a^* , it can be parameterised as a DNN and learned using stochastic gradient descent algorithms.

Training/learning process will repeatedly execute policy evaluation and policy improvement. In the policy evaluation, the Q-value in (10) is computed by applying a Bellman operation $Q_\pi(x_k, a_{l,k}) = \mathcal{T}^\pi Q_\pi(x_k, a_{l,k})$ where

$$\mathcal{T}^\pi Q_\pi(x_k, a_{l,k}) = \mathcal{C}_k + \gamma \mathbb{E}_{x_{k+1}} [\mathbb{E}_\pi [Q_\pi(x_{k+1}, a_{k+1})]], \quad (12)$$

where $Q_\pi(x_k, a_{l,k}) = Q_\pi(x_k, a_k) + \alpha \ln(\pi(a_k | x_k))$.

In the policy improvement, the policy is updated by

$$\pi_{\text{new}} = \arg \min_{\pi' \in \Pi} \mathcal{D}_{\text{KL}} \left(\pi'(\cdot | x_k) \left\| \frac{e^{-\frac{1}{\alpha} Q^{\pi_{\text{old}}}(x_k, \cdot)}}}{Z^{\pi_{\text{old}}}} \right. \right), \quad (13)$$

where π_{old} denotes the policy from the last update, $Q^{\pi_{\text{old}}}$ is the Q-value of π_{old} , \mathcal{D}_{KL} denotes the Kullback-Leibler (KL) divergence, and $Z^{\pi_{\text{old}}}$ is a normalisation factor. The objective can be transformed into

$$\pi^* = \arg \min_{\pi \in \Pi} \mathbb{E}_\pi [\alpha \ln(\pi(a_k | x_k)) + Q(x_k, a_k)]. \quad (14)$$

More details can be found in [33].

C. Data-based Stability Analysis

The convergence of bounded estimate error \tilde{x}_k is essentially equivalent to show the stability of (6). In this paper, we are interested in establishing the stability theorem by only using samples $\{\tilde{x}_{k+1}, \tilde{x}_k, a_k\}$, $\forall k$. The most useful and general approach for studying a dynamical system's stability is the Lyapunov method [34]–[36]. In Lyapunov method, a suitable “energy-like” Lyapunov function $\mathcal{L}(\tilde{x}_k)$ (for succinctness $\mathcal{L}(k)$ is used in the following context) is selected. Its derivative along the system trajectories is ensured to be negative semi-definite, i.e., $\mathcal{L}(k+1) - \mathcal{L}(k) \leq 0$ for all time instants and states, so that the state goes in the direction of decreasing the value of Lyapunov function and eventually converges to the origin or a sub-level set of the Lyapunov function. In this subsection, such a function is introduced to analyse the stability of the estimate error dynamical system (6). Unlike the model-based stability analysis literature, we will learn a Lyapunov function instead of an explicit expression regardless of the degree of nonlinearity of the system and the time-consuming human expert design. The Lyapunov candidate $\mathcal{L}(k)$ can be chosen as the Q-function $Q_\pi(\tilde{x}_k, a_k)$ [25]–[28]. It is well-known that the Q-function $Q_\pi(\tilde{x}_k, a_k)$ is related to the cost \mathcal{C}_k . Thus, there always exist a positive function

$$\mathcal{L}(k) = \mathcal{C}_k + \delta_k = Q_\pi(\tilde{x}_k, a_k) \quad (15)$$

where $Q_\pi(\tilde{x}_k, a_k)$ can be parameterised by a DNN. Here, $\delta_k > 0$ should be satisfied due to the property of the Q-function, and it should be also non-increasing. Once the trace of the covariance of estimate error converges, the cost \mathcal{C}_k and Q-function both converge as well, as a result δ_k will converge to a constant number. We first prove the stability theorem by exploiting the function $\mathcal{L}(k)$ and the characteristic of δ_k . The details of the learning algorithm will be discussed in Section IV. We need the following assumption and lemma for the proof.

Assumption 1. *A Markov chain induced by a policy π is ergodic with a unique distribution probability $q_\pi(\tilde{x}_k)$ with $q_\pi(\tilde{x}_k) = \lim_{k \rightarrow \infty} \mathcal{P}(\tilde{x}_k | \rho, \pi, k)$, where ρ denotes the distribution of starting states.*

Remark 2. *The verification of ergodicity is, in general, an open question and also in the long history of ergodic theory. Many systems have proved to be ergodic in physics, statistic mechanics, economics [37], [38]. The study of ergodicity of various systems and its verification composes a significant branch of mathematics. If the transition probability is known for all states, the validation is possible but requires an extensive resource of computation power to enumerate through the state space. The existence of the stationary state distribution is generally assumed to hold in the RL literature [39]–[41]. In this paper, based on the ergodicity assumption, we focus on analysing the stability of such systems and developing an algorithm to find the filter gain.*

Before proving the main theorem, we also need the following Lemma

Lemma 1. [42] *(Lebesgue’s Dominated convergence theorem) Suppose $f_n : \mathcal{R} \rightarrow [-\infty, +\infty]$ (Lebesgue) measurable func-*

tions such that the point-wise limit $f(x) = \lim_{n \rightarrow \infty} f_n(x)$ exists. Assume there is an integrable function $g : \mathcal{R} \rightarrow [-\infty, +\infty]$ with $|f_n(x)| \leq g(x)$ for each $x \in \mathcal{R}$, then f is integrable (in the Lebesgue sense) and

$$\lim_{n \rightarrow \infty} \int_{\mathcal{R}} f_n d\mu = \int_{\mathcal{R}} \lim_{n \rightarrow \infty} f_n d\mu = \int_{\mathcal{R}} f d\mu.$$

Based on Assumption 1 and Lemma 1, we prove our main theorem in the following.

Theorem 1. *If there exist a function $\mathcal{L}(k) \geq 0$, and constants $\alpha_1 \geq 0$, $\alpha_2 > 0$, and $\beta \geq 0$ such that the following inequalities hold*

$$\begin{aligned} \alpha_1 \mathcal{C}_k &\leq \mathcal{L}(k) \leq \alpha_2 \mathcal{C}_k, \\ \mathbb{E}_{\tilde{x}_k \sim \mu_\pi} [\mathbb{E}_{\tilde{x}_{k+1} \sim \mathcal{P}_\pi} [\mathcal{L}(k+1)] - \mathcal{L}(k)] & \\ &\leq -\beta \mathbb{E}_{\tilde{x}_k \sim \mu_\pi} \{\|\tilde{x}_k\|^2\} + \delta_k, \quad \forall k \in \mathcal{Z}_+. \end{aligned} \quad (16)$$

Then the estimate error \tilde{x}_k is guaranteed to be exponentially bounded in mean square, i.e.,

$$\mathbb{E}_{\tilde{x}_k \sim \mu_\pi} [\|\tilde{x}_k\|^2] \leq \sigma^k \mathbb{E}_{\tilde{x}_0 \sim \mu_\pi} [\|\tilde{x}_0\|^2] + p, \quad (17)$$

where

$$\mu_\pi(\tilde{x}_k) \triangleq \lim_{N \rightarrow \infty} \frac{1}{N} \sum_{k=0}^N \mathcal{P}(\tilde{x}_k | \rho, \pi, k)$$

is the estimate error distribution, and $p = \sum_{l=0}^{k-1} \sigma^{k-l-1} \delta_l$, $\sigma \in (0, 1)$.

Proof. The existence of the sampling distribution $\mu_\pi(\tilde{x}_k)$ is guaranteed by the existence of $q_\pi(\tilde{x}_k)$. Since the sequence $\{\mathcal{P}(\tilde{x}_k | \rho, \pi, k), k \in \mathcal{Z}_+\}$ converges to $q_\pi(\tilde{x}_k)$ as k approaches ∞ , then by the Abelian theorem that if a sequence or function behaves regularly, then some average of it behaves regularly. We have the sequence $\left\{ \frac{1}{N} \sum_{k=0}^N \mathcal{P}(\tilde{x}_k | \rho, \pi, k), N \in \mathcal{Z}_+ \right\}$ also converges and $\mu_\pi(\tilde{x}_k) = q_\pi(\tilde{x}_k)$. Then, (16) can be rewritten as

$$\begin{aligned} &\int_{\mathcal{S}} \lim_{N \rightarrow \infty} \frac{1}{N} \sum_{k=0}^N \mathcal{P}(\tilde{x}_k | \rho, \pi, k) (\mathbb{E}_{\mathcal{P}_\pi(\tilde{x}_{k+1}|s)} [\mathcal{L}(k+1)] - \mathcal{L}(k)) d\tilde{x}_k \\ &\leq -\beta \mathbb{E}_{\tilde{x}_k \sim \mu_\pi} \|\tilde{x}_k\|^2 + \delta_k \end{aligned}$$

The left-hand-side of the above inequality can be derived as

follows:

$$\begin{aligned}
& \int_S \lim_{N \rightarrow \infty} \frac{1}{N} \sum_{k=0}^N P(\tilde{x}_k | \rho, \pi, k) \left(\int_S P_\pi(\tilde{x}_{k+1} | \tilde{x}_k) \mathcal{L}(k+1) d\tilde{x}_{k+1} - \mathcal{L}(k) \right) d\tilde{x}_k \\
&= \int_S \lim_{N \rightarrow \infty} \frac{1}{N} \sum_{k=0}^N P(\tilde{x}_k | \rho, \pi, k) \int_S P_\pi(\tilde{x}_{k+1} | \tilde{x}_k) \mathcal{L}(k+1) d\tilde{x}_{k+1} d\tilde{x}_k \\
&\quad - \int_S \lim_{N \rightarrow \infty} \frac{1}{N} \sum_{k=0}^N P(\tilde{x}_k | \rho, \pi, k) \mathcal{L}(k) d\tilde{x}_k \\
&= \int_S \lim_{N \rightarrow \infty} \frac{1}{N} \int_S \sum_{k=0}^N P(\tilde{x}_k | \rho, \pi, k) P_\pi(\tilde{x}_{k+1} | \tilde{x}_k) \mathcal{L}(k+1) d\tilde{x}_k d\tilde{x}_{k+1} \\
&\quad - \int_S \lim_{N \rightarrow \infty} \frac{1}{N} \sum_{k=0}^N P(\tilde{x}_k | \rho, \pi, k) \mathcal{L}(k) d\tilde{x}_k \\
&= \int_S \lim_{N \rightarrow \infty} \frac{1}{N} \mathcal{L}(k+1) d\tilde{x}_{k+1} \int_S \sum_{k=0}^N P(\tilde{x}_k | \rho, \pi, k) P_\pi(\tilde{x}_{k+1} | \tilde{x}_k) d\tilde{x}_k \\
&\quad - \int_S \lim_{N \rightarrow \infty} \frac{1}{N} \sum_{k=0}^N P(\tilde{x}_k | \rho, \pi, k) \mathcal{L}(k) d\tilde{x}_k \\
&= \int_S \lim_{N \rightarrow \infty} \frac{1}{N} \int_S \sum_{k=0}^N P(\tilde{x}_{k+1} | \rho, \pi, k+1) \mathcal{L}(k+1) d\tilde{x}_{k+1} \\
&\quad - \int_S \lim_{N \rightarrow \infty} \frac{1}{N} \sum_{k=0}^N P(\tilde{x}_k | \rho, \pi, k) \mathcal{L}(k) d\tilde{x}_k
\end{aligned} \tag{18}$$

Since $\mathcal{L}(k) \leq \alpha_2 \mathcal{C}_k$ and $P(\tilde{x}_k | \rho, \pi, k) \leq 1$, then $P(\tilde{x}_k | \rho, \pi, k) \mathcal{L}(k) \leq \alpha_2 \mathcal{C}_k$. Besides, the sequence $\left\{ \frac{1}{N} \sum_{k=0}^N P(\tilde{x}_k | \rho, \pi, k) \mathcal{L}(k) \right\}$ converges point-wise to the function $q_\pi(\tilde{x}_k) \mathcal{L}(k)$. According to the Lebesgue's dominated convergence theorem (Lemma 1), it follows from (18) that :

$$\begin{aligned}
& \int_S \lim_{N \rightarrow \infty} \frac{1}{N} \sum_{k=0}^N P(\tilde{x}_k | \rho, \pi, k) \left(\int_S P_\pi(\tilde{x}_{k+1} | \tilde{x}_k) \mathcal{L}(k+1) d\tilde{x}_{k+1} - \mathcal{L}(k) \right) d\tilde{x}_k \\
&= \int_S \lim_{N \rightarrow \infty} \frac{1}{N} \int_S \sum_{k=0}^N P(\tilde{x}_{k+1} | \rho, \pi, k+1) \mathcal{L}(k+1) d\tilde{x}_{k+1} \\
&\quad - \int_S \lim_{N \rightarrow \infty} \frac{1}{N} \sum_{k=0}^N P(\tilde{x}_k | \rho, \pi, k) \mathcal{L}(k) d\tilde{x}_k \\
&= \lim_{N \rightarrow \infty} \frac{1}{N} \left(\sum_{k=1}^{N+1} \mathbb{E}_{P(\tilde{x}_k | \rho, \pi, k)} \mathcal{L}(k) - \sum_{k=0}^N \mathbb{E}_{P(\tilde{x}_k | \rho, \pi, k)} \mathcal{L}(k) \right) \\
&= \lim_{N \rightarrow \infty} \frac{1}{N} \sum_{k=0}^N (\mathbb{E}_{P(\tilde{x}_{k+1} | \rho, \pi, k+1)} \mathcal{L}(k+1) - \mathbb{E}_{P(\tilde{x}_k | \rho, \pi, k)} \mathcal{L}(k)).
\end{aligned} \tag{19}$$

It further follows from (16) and (19) that

$$\begin{aligned}
& \mathbb{E}_{P(\tilde{x}_{k+1} | \rho, \pi, k+1)} \mathcal{L}(k+1) - \mathbb{E}_{P(\tilde{x}_k | \rho, \pi, k)} \mathcal{L}(k) \\
&\leq -\beta \mathbb{E}_{\tilde{x}_k \sim \mu_\pi} \{ \|\tilde{x}_k\|^2 \} + \delta_k
\end{aligned} \tag{20}$$

Given α_2 and β , there always exists a scalar σ such that the following equation holds

$$\left(\frac{1}{\sigma} - 1 \right) \alpha_2 - \frac{\beta}{\sigma} = 0. \tag{21}$$

Using (20) and (21), the following inequality can be derived

$$\begin{aligned}
& \frac{1}{\sigma^{\ell+1}} \mathbb{E}_{P(\tilde{x}_{\ell+1} | \rho, \pi, \ell+1)} \mathcal{L}(\ell+1) - \frac{1}{\sigma^\ell} \mathbb{E}_{P(\tilde{x}_\ell | \rho, \pi, \ell)} \mathcal{L}(\ell) \\
&\stackrel{(21)}{=} \frac{1}{\sigma^{\ell+1}} (\mathbb{E}_{P(\tilde{x}_{\ell+1} | \rho, \pi, \ell+1)} \mathcal{L}(\ell+1) - \mathbb{E}_{P(\tilde{x}_\ell | \rho, \pi, \ell)} \mathcal{L}(\ell)) \\
&\quad + \frac{1}{\sigma^\ell} \left(\frac{1}{\sigma} - 1 \right) \mathbb{E}_{P(\tilde{x}_\ell | \rho, \pi, \ell)} \mathcal{L}(\ell) \\
&\leq \frac{1}{\sigma^\ell} \left(-\frac{\beta}{\sigma} + \left(\frac{1}{\sigma} - 1 \right) \alpha_2 \right) \mathbb{E}_{\tilde{x}_k \sim \mu_\pi} \{ \|\tilde{x}_k\|^2 \} \\
&\quad + \frac{\delta_\ell}{\sigma^{\ell+1}}, \quad \forall \ell \geq 0,
\end{aligned}$$

which implies

$$\begin{aligned}
& \frac{1}{\sigma^{\ell+1}} \mathbb{E}_{P(\tilde{x}_{\ell+1} | \rho, \pi, \ell+1)} \mathcal{L}(\ell+1) - \frac{1}{\sigma^\ell} \mathbb{E}_{P(\tilde{x}_\ell | \rho, \pi, \ell)} \mathcal{L}(\ell) \\
&\leq \frac{\delta_\ell}{\sigma^{\ell+1}}.
\end{aligned} \tag{22}$$

To sum the above inequality from $\ell = 0, 1, \dots, k-1$ yields

$$\begin{aligned}
& \frac{1}{\sigma^k} \mathbb{E}_{P(\tilde{x}_k | \rho, \pi, k)} \mathcal{L}(k) - \mathbb{E}_{P(\tilde{x}_0 | \rho, \pi, 0)} \mathcal{L}(0) \\
&\leq \sum_{\ell=0}^{k-1} \frac{\delta_\ell}{\sigma^{\ell+1}},
\end{aligned}$$

which implies

$$\mathbb{E}_{\tilde{x}_k \sim \mu_\pi} \left[\|\tilde{x}_k\|^2 \right] \leq \sigma^k \mathbb{E}_{\tilde{x}_0 \sim \mu_\pi} \left[\|\tilde{x}_0\|^2 \right] + p.$$

where the scalar constant p is an upper bound of the sequence $\left\{ \sum_{t=0}^{k-1} \sigma^{k-t-1} \delta_t, k \geq 0 \right\}$. Since $\sigma \in (0, 1)$ and δ_k is non-increasing, we can conclude that the upper bound p exists. Thus, the estimate error is exponentially bounded in mean square, which completes the proof. \square

IV. REINFORCEMENT LEARNING FILTER DESIGN

In this section, we will discuss the reinforcement learning algorithm design and implementation. We will design the algorithm based on the actor-critic RL algorithms which are widely used in continuous control tasks [32]. In actor-critic RL, typically DNNs are used to approximate the ‘‘critic’’ and the ‘‘actor’’. In the following, we will introduce how to incorporate convergence conditions derived in Subsection III-C into such algorithm architectures. Then the convergence of the algorithm will be analysed.

A. Deep neural networks approximation

DNNs approximation are used due to the continuous state and action spaces in this paper. The DNNs are constructed by fully connected multiple layer perceptrons (MLP), in which the rectified linear unit (ReLU) nonlinearities are chosen as the activation functions [43]. The ReLU nonlinearities are defined as $\rho(z) = \max\{z, 0\}$ when z is a scalar. Given a vector $z = [z_1, \dots, z_n]^\top \in \mathbb{R}^n$, then $\rho(z) = [\rho(z_1), \dots, \rho(z_n)]^\top$. An example of a MLP with two hidden layers is described as

$$\underline{\text{MLP}}_w^2(z) = w_2 \left[\rho \left(w_1 \left[\rho \left(w_0 \begin{bmatrix} z \\ 1 \end{bmatrix} \right), 1 \right] \right)^\top, 1 \right]^\top, \tag{23}$$

where $[z^\top, 1]^\top$ is a vector composed of z and a constant bias 1, the superscript “2” denotes the total number of hidden layers, the subscript “w” denotes the parameter set to be trained in a MLP with $w = \{w_0, w_1, w_2\}$, and w_0, w_1 , and w_2 are weight matrices with appropriate dimensions.

If there is a set of inputs $z = \{z_1, \dots, z_L\}$ for the MLP in (23) with z_1, \dots, z_L denoting vector signals, we have

$$\underline{\text{MLP}}_w^2(z) = \underline{\text{MLP}}_w^2([z_1^\top, \dots, z_L^\top]^\top). \quad (24)$$

Besides, $\underline{\text{MLP}}_w^2(z_1, z_2) = \underline{\text{MLP}}_w^2([z_1^\top, z_2^\top]^\top)$ for two vector inputs z_1 and z_2 . If $z_1 = \{z_{11}, \dots, z_{1L}\}$ is a set of vectors, $\underline{\text{MLP}}_w^2(z_1, z_2) = \underline{\text{MLP}}_w^2([z_{11}^\top, \dots, z_{1L}^\top, z_2^\top]^\top)$.

In this paper, the constructed MLPs are used to approximate the “critic” $Q_\pi(\tilde{x}_k, a_k)$ and the “actor” $\pi(a_k|\tilde{x}_k)$. We respectively use θ and ϕ to parameterise $Q(\tilde{x}_k, a_k)$ and $\pi(a_k|\tilde{x}_k)$, i.e., $Q_\theta(\tilde{x}_k, a_k)$ and $\pi_\phi(a_k|\tilde{x}_k)$. As discussed in Section III-C, the Q-function $Q(\tilde{x}_k, a_k)$ is regarded as a Lyapunov candidate $\mathcal{L}(k)$ in our paper. Namely, the “critic” is the Lyapunov function. In the following context, we replace $Q(\tilde{x}_k, a_k)$ with $\mathcal{L}(k)$, and $Q_\theta(\tilde{x}_k, a_k)$ with $\mathcal{L}_\theta(k)$. The direct output of the constructed MLP may not satisfy the requirements of a Lyapunov function $\mathcal{L}(k)$, for example, $\mathcal{L}(k) > 0, \forall k \geq 0$, so it is necessary to modify the representation of MLP. Following (23) and (24), the Lyapunov function approximation $\mathcal{L}_\theta(k)$ is chosen as

$$\mathcal{L}_\theta(k) = \left(\underline{\text{MLP}}_\theta^{K_1}(\tilde{x}_k) \right)^2, \quad (25)$$

where $\theta = \{\theta_0, \dots, \theta_{K_1}\}$ with θ_i denoting the weight matrices of proper dimensions, $0 \leq i \leq K_1$. The DNN for \mathcal{L}_θ is illustrated in Fig. 1.

The filter gain a_k is also approximated using a MLP. The approximated filter gain of a_k with a parameter set ϕ is

$$a_\phi = \underline{\text{MLP}}_\phi^{K_2}(\tilde{x}_k). \quad (26)$$

The illustration of a_ϕ is given in Figure 1. In the learning setup, there are two outputs for the MLP in (26). One is the control law a_ϕ , the other one is σ_ϕ that is the standard deviation (SD) of the exploration noise [33]. According to (8), the parameterised policy π_ϕ in our learning is

$$\pi_\phi = \mathcal{N}(a_\phi(\tilde{x}), \sigma_\phi^2). \quad (27)$$

B. Lyapunov reinforcement learning filter (LRLF)

The actor-critic RL training process is depicted in Fig. 2. In the training process, the dynamic system (1) and the state estimator to be trained (2) repeatedly run to collect the data, which is restored as the replay memory \mathcal{M} . After \mathcal{M} is collected, the policy evaluation and improvement are executed by randomly sampling a batch of data in \mathcal{M} . Then, the improved policy $\pi_\phi(a_k|\tilde{x}_k)$ is applied to the state estimator to generate data until $\mathcal{L}_\theta(k)$ converges.

In the learning stage, the policy is obtained by repeatedly executing the policy evaluation and policy improvement. For the policy evaluation, it starts from any function $\mathcal{L} : \mathcal{S} \times \mathcal{A} \rightarrow \mathcal{R}$ under a fixed policy π , and repeatedly applies a Bellman backup operator \mathcal{T}^π , which is defined as

$$\mathcal{T}^\pi \mathcal{L}_\pi(k) = \mathcal{C}_k + \gamma \mathbb{E}_{\tilde{x}_{k+1}} [\mathbb{E}_\pi [\mathcal{L}_\pi(k+1)]]. \quad (28)$$

At each policy evaluation step, the policy $\pi_\phi(a_k|\tilde{x}_k)$ should minimise the following Bellman residual equation

$$\mathcal{J}_\mathcal{L}(\theta) = \mathbb{E}_{(\tilde{x}_k, a_k \sim \mathcal{M})} \left\{ \frac{1}{2} (\mathcal{L}_\theta(k) - \mathcal{L}_{\text{target}})^2 \right\},$$

where $(\tilde{x}_k, a_k \sim \mathcal{M})$ represents the operation that randomly takes (\tilde{x}_k, a_k) from the memory \mathcal{M} , and

$$\mathcal{L}_{\text{target}} = \mathcal{C}_k + \gamma \mathbb{E}_{\tilde{x}_{k+1}} [\mathbb{E}_{\bar{\theta}} [\mathcal{L}_{\bar{\theta}}(k+1) + \alpha \ln(\pi_\phi)]],$$

with $\bar{\theta}$ being the target network parameter.

We can obtain the following by using stochastic gradient descent:

$$\nabla_\theta \mathcal{J}_\mathcal{L}(\theta) = \sum \frac{\nabla_\theta \mathcal{L}_\theta}{|\mathcal{B}|} (\mathcal{L}_\theta(k) - \mathcal{L}_{\text{target}}),$$

where $|\mathcal{B}|$ denotes the batch size.

At the policy improvement stage, the improved policy should guarantee the Lyapunov inequality in Theorem 1 holds. Thus, the policy is updated as

$$\pi_{\text{new}} = \arg \min_{\pi' \in \Pi} \mathcal{D}_{\text{KL}} \left(\pi'(\cdot|\tilde{x}_k) \parallel \frac{e^{-\frac{1}{\alpha} \mathcal{L}_{\pi_{\text{old}}}(\tilde{x}_k, \cdot)}}}{Z_{\pi_{\text{old}}}(\tilde{x}_k)} \right) \quad (29)$$

$$\text{s.t. } \mathcal{L}_\theta(k+1) - \mathcal{L}(k) \leq -\beta \text{Tr}(\tilde{x}_k \tilde{x}_k^\top) + \delta_k,$$

where Π is the policy set, π_{old} is the last updated policy, $\mathcal{L}_{\pi_{\text{old}}}$ is the action value function of π_{old} , \mathcal{D}_{KL} means the Kullback-Leibler divergence, and $Z_{\pi_{\text{old}}}$ is a partition function which is introduced to normalise the distribution.

Remark 3. Different from the SAC algorithm, the Lyapunov constraint, that is, $\mathcal{L}_\theta(k+1) - \mathcal{L}(k) \leq -\beta \text{Tr}(\tilde{x}_k \tilde{x}_k^\top) + \delta_k$ is considered when the policy improvement step is executed. In this way, we can guarantee that the estimate error always converges to a positive constant in mean square, which is proved in Theorem 1.

Then we can rewrite (29) as

$$\pi_{\text{new}} = \arg \min_{\pi \in \Pi} \mathbb{E} [\alpha \ln(\pi(a_k|\tilde{x}_k)) + \mathcal{L}(k)] \quad (30)$$

$$\text{s.t. } \mathcal{L}_\theta(k+1) - \mathcal{L}(k) \leq -\beta \text{Tr}(\tilde{x}_k \tilde{x}_k^\top) + \delta_k.$$

For the optimisation of (30), the Lagrangian multiplier can be introduced to deal with the constraint. Thus, (30) can be further described as

$$\begin{aligned} \pi_{\text{new}} = \arg \min_{\pi \in \Pi} \mathbb{E} [\alpha \ln(\pi(a_k|\tilde{x}_k)) + \mathcal{L}(k)] \\ + \lambda (\mathcal{L}_\theta(k+1) - \mathcal{L}(k) + \beta \text{Tr}(\tilde{x}_k \tilde{x}_k^\top) - \delta_k), \end{aligned} \quad (31)$$

where λ is a Lagrangian multiplier.

Based on the setup of RL, the policy improvement in (31) is converted into finding π^* by minimising the following function

$$\mathcal{J}_\pi(\phi) = \mathbb{E}_{(\tilde{x}_k, a_k \sim \mathcal{M})} \{ \alpha \ln(\pi_\phi) + \mathcal{L}_\theta(k) \},$$

whose gradient in terms of ϕ is derived as

$$\nabla_\phi \mathcal{J}_\pi(\phi) = \sum \frac{(\alpha \nabla_{a_k} \ln \pi_\phi + \nabla_{a_k} \mathcal{L}_\theta(k)) \nabla_\phi a_\phi + \alpha \nabla_\phi \ln \pi_\phi}{|\mathcal{B}|}.$$

For the temperature α , it is updated by minimising the following function

$$\mathcal{J}_\alpha = \mathbb{E}_\pi \{ -\alpha \ln \pi(a_k|\tilde{x}_k) - \alpha \mathcal{H} \},$$

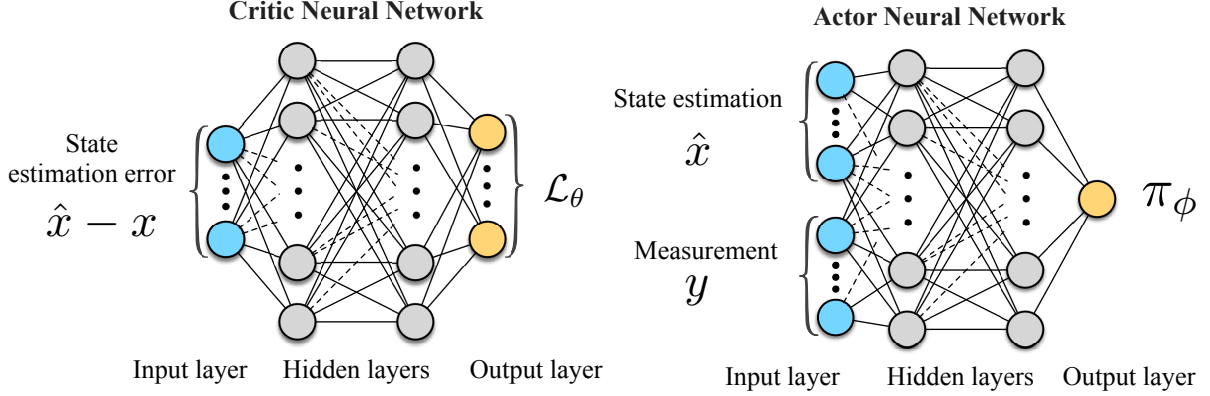


Fig. 1: Approximation of \mathcal{L}_θ and π_ϕ using MLP

where \mathcal{H} is a target entropy.

For the Lagrangian multiplier λ , it is learned by maximising

$$\mathcal{J}(\lambda) = \mathbb{E} [\mathcal{L}_\theta(k+1) - \mathcal{L}(k) + \beta \text{Tr}(\tilde{x}_k \tilde{x}_k^\top) - \delta_k].$$

Our algorithm is implemented based on SAC algorithm [33], in which $\iota_{\mathcal{L}}, \iota_\pi, \iota_\alpha$, and ι_λ are the positive learning rates, and $\tau > 0$ is a constant scalar. The optimal parameters for the DNN in (25) and (26) will be learned, and the filter gain policy will be approximated by π_{ϕ^*} from which action will be sampled. During inference, the mean value of π_{ϕ^*} will be deployed since the policy is often assumed to be Gaussian distributed in SAC [33].

The inference procedure is illustrated in Fig. 3. The learned policy is deployed to tune the error $y_{k+1} - g(f(\hat{x}_k))$ in the estimator. We sample the measurement output signal y_{k+1} from the real system. Then, the estimator starts to estimate states for the real system.

Remark 4. Bayesian nonlinear filtering methods such as the EKF, UKF, PF adjust the estimator gains or sampling weights via online computation. The proposed LRLF is trained offline, and the filter gain is approximated by a DNN which will be deployed directly for online applications. In this paper, like other methods, the training needs full knowledge of the mathematical model, i.e., (1). It should also be noted that the filter (2) is trained by only using the samples simulated from (1) instead of any other assumptions on the model. In other words, the mathematical model is a simulator, and our training is performed in a model-free manner. In Figs. 2 and 3, the statistical information of the system's noise such as the covariance is not directly used by the LRLF, which is different from the EKF, UKF and PF where such statistical information is used explicitly.

C. Algorithm convergence analysis

Next, a lemma is given to show that the policy evaluation can guarantee the action value function to converge. Since the proof is standard, it is omitted here. Readers can refer to [33] for more details.

Lemma 2. (Policy evaluation) Consider the backup operator \mathcal{T}^π in (28) and define $\mathcal{L}^{t+1}(k) \triangleq \mathcal{T}^\pi \mathcal{L}^t(k)$. The sequence

Algorithm 1 Lyapunov-Based Reinforcement Learning Filter Algorithm (LRLF)

- 1: Set the initial parameters θ for the Lyapunov function \mathcal{L}_θ , ϕ for the filtering policy π_ϕ , λ for the Lagrangian multiplier, α for the temperature parameter, and the replay memory \mathcal{M}
 - 2: Set the target parameter $\bar{\theta}$ as $\bar{\theta} \leftarrow \theta$
 - 3: **while** Training **do**
 - 4: **for** each data collection step **do**
 - 5: Choose a_k using $\pi_\theta(a_k|\tilde{x}_k)$
 - 6: Run the system (1) and the filter system (2) and collect data \tilde{x}_k
 - 7: $\mathcal{M} \leftarrow \mathcal{M} \cup \tilde{x}_k$
 - 8: **end for**
 - 9: **for** each gradient step **do**
 - 10: $\theta \leftarrow \theta - \iota_{\mathcal{L}} \nabla_\theta \mathcal{J}_{\mathcal{L}}(\theta)$,
 - 11: $\phi \leftarrow \phi - \iota_\pi \nabla_\phi \mathcal{J}_\pi(\phi)$
 - 12: $\alpha \leftarrow \alpha - \iota_\alpha \nabla_\alpha \mathcal{J}_\alpha(\alpha)$
 - 13: $\lambda \leftarrow \lambda - \iota_\lambda \nabla_\lambda \mathcal{J}_\lambda(\lambda)$
 - 14: $\phi_{\bar{\theta}} \leftarrow \tau\theta + (1 - \tau)\phi_{\bar{\theta}}$,
 - 15: **end for**
 - 16: **end while**
 - 17: Output optimal parameters θ^* , ϕ^* , λ^* , and α^*
-

$\mathcal{L}^{t+1}(k)$ can converge to a soft value \mathcal{L}^π of the policy π as the iteration $t \rightarrow \infty$.

For policy improvement, a lemma is given to show that the updated policy is better than the last one.

Lemma 3. (Policy improvement) Considering the last updated policy π_{old} and the new policy π_{new} to be obtained from (30), $\mathcal{L}^{\pi_{new}(k)} \leq \mathcal{L}^{\pi_{old}(k)}$ holds, $\forall \tilde{x}_k \in \mathcal{S}$ and $\forall a_k \in \mathcal{A}$.

Proof. According to (30), we can obtain

$$\begin{aligned} \mathbb{E}_{\pi_{new}} [\alpha \ln(\pi_{new}(a_k|\tilde{x}_k)) + \mathcal{L}_{\pi_{old}}(k)] &\leq \\ \mathbb{E}_{\pi_{old}} [\alpha \ln(\pi_{old}(a_k|\tilde{x}_k)) + \mathcal{L}_{\pi_{old}}(k)], \end{aligned}$$

which implies

$$\mathbb{E} [\mathcal{L}_{\pi_{old}} + \alpha \ln(\pi_{new}(a_k|\tilde{x}_k))] \leq V_{\pi_{old}}(\tilde{x}_k). \quad (32)$$

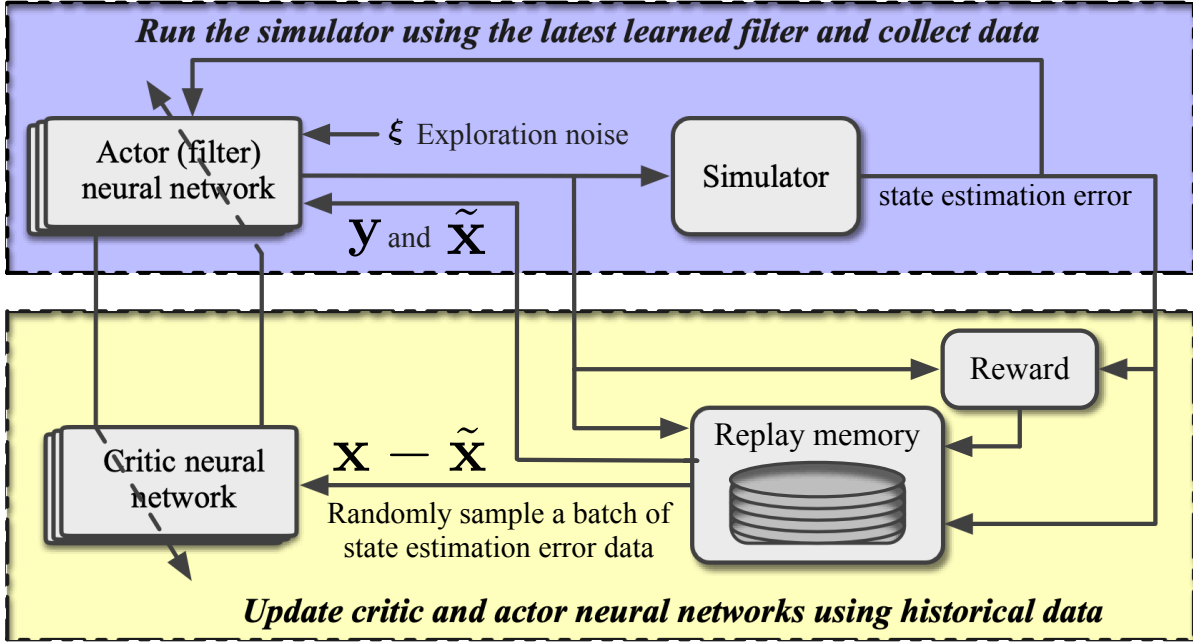


Fig. 2: Offline training process of LRLF

Then, the following inequality holds

$$\begin{aligned}
 \mathcal{L}_{\pi_{\text{old}}}(k) &= \mathcal{C}_k + \gamma \mathbb{E}_{\tilde{x}_{k+1}} [V_{\pi_{\text{old}}}(\tilde{x}_k)] \\
 &\geq \mathcal{C}_k + \gamma \mathbb{E}_{\tilde{x}_{k+1}} [\mathbb{E}_{\pi_{\text{new}}} [\\
 \mathcal{L}_{\pi_{\text{old}}}(k+1) &+ \alpha \ln(\pi_{\text{new}}(a_{k+1}|\tilde{x}_{k+1}))]] \\
 &\vdots \\
 &\geq \mathcal{L}_{\pi_{\text{new}}}(k),
 \end{aligned}$$

where (32) is repeatedly used and hence omitted. It completes the proof. \square

Next, a theorem is derived to show that the convergence of Algorithm 1 can be guaranteed.

Theorem 2. Define π_i ($i = 1, 2, \dots, \infty$) as the policy obtained at the i -th policy improvement step, starting from any policy $\pi_0 \in \Pi$, where Π is the policy set, then π_i will converge to an optimal policy π^* , ensuring $\mathcal{L}_{\pi^*}(k)$ converges to its minimal value as $k \rightarrow \infty$.

Proof. Based on Lemma 3, we know that the policy can achieve a better estimate performance after each policy improvement, that is, $\mathcal{L}_{\pi_i}(k) \leq \mathcal{L}_{\pi_{i-1}}(k)$. By repeatedly executing the policy evaluation and policy improvement, a policy π_i can converge to π^* as $i \rightarrow \infty$. Thus, $\mathcal{L}_{\pi^*}(k)$ can converge based on the conclusion in Lemma 2. \square

V. SIMULATION

The experiment setup for the LRLF is a three-stage procedure. First, a number of N estimation policies are trained for different initial conditions and noise is sampled from a known distribution. During training, the simulator will generate sample trajectories $\{x_k^i, y_k^i, i = 1, \dots, I, k = 1, \dots, K\}$, where I, K

are the number of training trajectories and that of the trajectory length respectively. Second, the estimation performance of each DRL-based state estimator (2) will be evaluated by running M Monte Carlo simulations, again for different initial conditions and noise sampled from a known distribution. Finally, the state estimator with the lowest trace of estimate error covariance during inference (unless diverged) will be deployed online and used for comparison with other nonlinear filtering algorithms.

We first consider a free-pendulum tracking example widely used as a benchmark for nonlinear state estimation [4], [12], [44]. The pendulum has unity mass of 1 kg and length of 1 m. The discrete-time dynamics of the pendulum is given as follows:

$$\begin{bmatrix} x_{1,k+1} \\ x_{2,k+1} \end{bmatrix} = \begin{bmatrix} x_{1,k} + x_{2,k}\delta t \\ x_{2,k} - g \sin(x_{1,k})\delta t \end{bmatrix} + w_k \quad (33)$$

where $x_{1,k} = \theta_k$, $x_{2,k} = \omega_k$ are the angle and angle velocity of the pendulum at time instant k , respectively, δt is the sampling time and set as 0.1 second in the simulation. The process noise w_k is Gaussian distributed as

$$w_k \sim \mathcal{N}\left(\begin{bmatrix} 0 \\ 0 \end{bmatrix}, \begin{bmatrix} \frac{1}{3}(\delta t)^3 q_1 & \frac{1}{2}(\delta t)^2 q_1 \\ \frac{1}{2}(\delta t)^2 q_1 & \delta t q_1 \end{bmatrix}\right), q_1 = 0.01$$

The measurement equation is given as:

$$y_k = \sin(x_{1,k}) + v_k \quad (34)$$

where the measurement noise is also Gaussian distributed with $v_k \sim \mathcal{N}(0, 0.01)$. Since the scalar measurement solely depends on the angle (x_1), the estimate of the latent state x_2 has to be reconstructed using the cross-correlation information between the angle and the angular velocity in the dynamics (33).

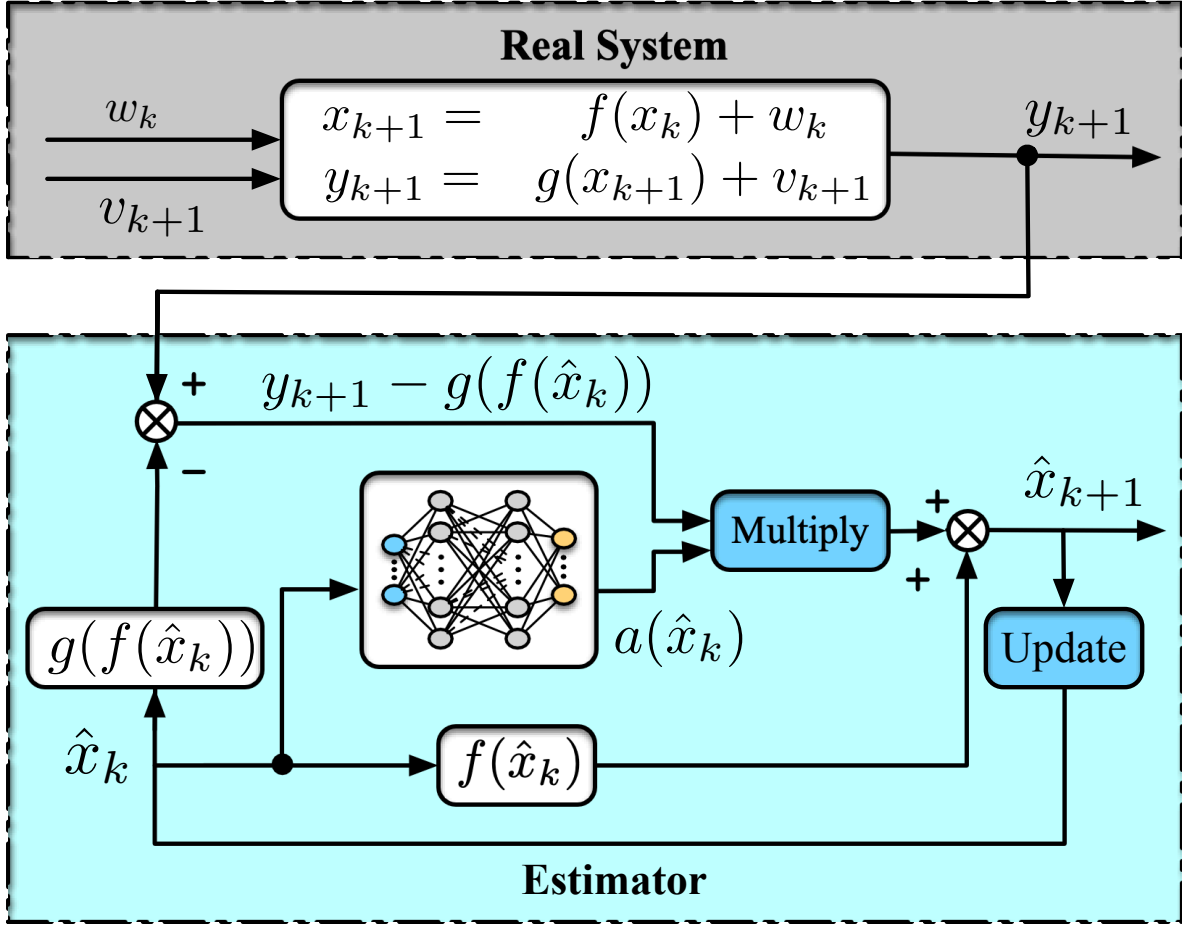


Fig. 3: Estimator structure

To test if the estimate error of LRLF converges regardless of the initial state and estimate, for each trajectory in the training, the initial state were sampled from uniform distribution:

$$\begin{aligned} \theta(0) &\sim \mathcal{U}[-0.5\pi, 0.5\pi], \\ \omega(0) &\sim \mathcal{U}[-0.5\pi, 0.5\pi], \end{aligned} \quad (35)$$

and the initial estimate was sampled from uniform distribution:

$$\begin{aligned} \hat{\theta}(0) &\sim \mathcal{U}[-0.25\pi + \theta(0), 0.25\pi + \theta(0)], \\ \hat{\omega}(0) &\sim \mathcal{U}[-0.25\pi + \omega(0), 0.25\pi + \omega(0)]. \end{aligned} \quad (36)$$

We compared LRLF with three other classic nonlinear Bayesian estimation algorithms, the EKF, UKF, and PF (10^3 and 10^4 particles respectively) [4]. The same initial state and state estimate in (35) and (36) were used for all estimation algorithms.

In the training, each trajectory has $K = 100$ data points (10 seconds simulation of (33)). We trained $N = 10$ policy networks and evaluated each network for $M = 500$ Monte Carlo simulations. The training details are give as follows:

For the LRLF, there are two networks: the policy network and the Lyapunov critic network. We use a fully-connected MLP with one hidden layer for the policy network, outputting the mean and SD of a Gaussian distribution. As mentioned in section IV, it should be noted that the output of the Lyapunov critic network is a square term, which is always

TABLE I: Hyperparameters of LRLF

Hyperparameters	Pendulum	Vehicle
Time horizon K	100	100
Minibatch size	256	256
Actor learning rate	1e-4	1e-4
Critic learning rate	3e-4	3e-4
Lyapunov learning rate	3e-4	3e-4
Target entropy	NaN	NaN
Soft replacement(τ)	0.005	0.005
Discount(γ)	0.995	0.995
α_3	0.1	0.1
Structure of a_ϕ	(32,16)	(32,16)
Structure of L_θ	(64,32)	(64,32)

non-negative. More specifically, we use a fully-connected MLP with one hidden layer and one output layer with different units as in Table I, outputting the feature vector Q_θ (see Fig. 1). The Lyapunov critic function is obtained by $L_c(s, a) = Q_\theta^\top(s, a)Q_\theta(s, a)$. All the hidden layers use ReLu activation function, and we adopt the same invertible squashing function technique as [33] to the output layer of the policy network.

The proposed LRLF was evaluated for the following aspects:

- 1) Algorithm convergence: does the proposed training algorithm converge with random initial states and estimate initialisation?
- 2) Estimate error convergence: does the estimate error

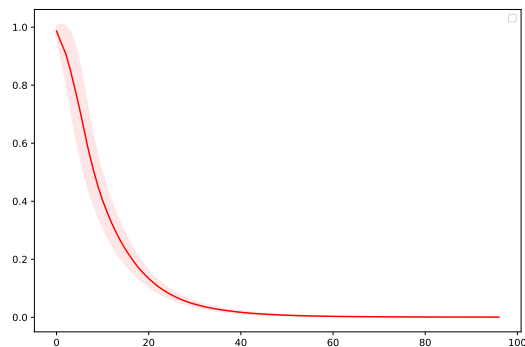


Fig. 4: The value of Lagrange multiplier λ during the training of LAC policies. The Y-axis indicates the value of λ and the X-axis indicates the total time steps. The shadowed region shows the 1-SD confidence interval over 10 randomly training policies.

variance converge compared with other state estimation algorithms?

- 3) Performance comparison: how does the proposed LRLF perform compared with other state estimation algorithms under various initial state conditions?
- 4) Robustness to uncertainty: how do the trained estimator perform during inference when faced with uncertainties unseen during training, such as noise with covariance shift and randomly-occurring missing measurement?

A. Algorithm convergence

We will validate the convergence guarantee by checking the values of Lagrange multipliers. When the Lyapunov constraint in (31) is satisfied, the parameter λ should continuously decrease to zero. In Fig. 4, the value of λ during training is demonstrated. In all training trials of the ten policy networks, λ converges to zero eventually, which implies the state estimate's convergence guarantee.

B. Estimation performance

The proposed LRLF is compared with the EKF, UKF and PF. For each method, a number of 500 Monte Carlo tests were run with random initial state given in (35) and (36). The average value and SD of estimate error \tilde{x}_k are illustrated in the left column of Fig. 5 (see Figs. 5(a, d, g, j, m)) for EKF, UKF, PF and LRLF. These comparisons show that only the PF with a larger number of particles (10^4) has comparable performance with the LRLF.

To verify estimation performance of the LRLF for nonlinear systems with non-Gaussian noise, we tested the LRLF over three typical non-Gaussian distributions as shown in Fig. 6. Specifically, the measurement noise v_k of the pendulum model in (33)-(34) is assumed to take three kinds of non-Gaussian probability distributions: 1) a Gaussian distribution $\mathcal{N}(0, 0.01)$ truncated between the interval $[0, 1]$; 2) a uniform distribution at the interval $[-0.3, 0.3]$; or 3) an exponential distribution with the PDF $p(w_k) = \begin{cases} 0.04 \exp(-0.04w_k) & \text{if } w_k \geq 0 \\ 0 & \text{if } w_k < 0 \end{cases}$. A number of 500 Monte Carlo simulations with random initial

state in (35) and (36) were test for each kind of measurement noise. The average value and SD of estimate error \tilde{x}_k are illustrated in Fig. 7. It is found that the LRLF still generates state estimate with bounded estimate errors under all the three kinds of non-Gaussian noises.

C. Robustness of the estimator

We considered the robustness of state estimators for two scenarios. (1) Against larger measurement noise: in the inference, the measurement noise variance increases from 0.01 to 0.1. (2) Against missing measurement: y_k is sampled/contaminated randomly with Bernoulli distribution, in which $p(\text{missing}) = p(\text{not missing}) = 0.5$. This means half of the measurements are not received/set to zeros during inference.

1) *Larger measurement noise*: Similarly, we run 500 Monte Carlo tests with random initial states and initial state estimates given in (35)-(36) for each state estimator. The average value and variance of estimate error \tilde{x}_k are illustrated in Figs.5 (b), (e), (h), (k), (n). From Figs.5 (b), (e), (h), it can be found that under a large measurement noise with variance 0.1, the estimates of the EKF, UKF and PF (10^3 particles) all diverge, while the estimate error of our proposed LRLF and PF (10^4 particles) increase compared with those under noise with variance 0.01 but are both still bounded, as shown in Figs.5 (k), (n). The LRLF produces comparable estimation performance to the computationally expensive PF with 10^4 particles. It is worth pointing out that our proposed state estimator, though trained under noise with the variance of 0.01, still works well under a changing noise level, showing its robustness to the covariance shift of system noise. From the left and middle column in Fig. 5, it is found that the EKF, UKF and PF (10^3 particles) have poor performance when measurement noise is large.

2) *Missing measurement*: Missing measurement is a common network-induced phenomenon and has been extensively investigated in state estimation for decades [45], [46]. In our experiment, the measurement are sampled/contaminated randomly with a Bernoulli distribution, e.g., $p(\text{missing}) = p(\text{no missing}) = 0.5$. The average value and variance of estimate error \tilde{x}_k are illustrated in Fig. 5 (c), (f), (i), (l), (o). It is found that the EKF, UKF and PF with 10^3 particles all diverge, LRLF has comparable performance as the PF with 10^4 particles. These comparisons imply that LRLF is robust to randomly missing measurement.

D. A linear system case study

We also consider the linear systems, to compare with the classic Kalman filter which is known to be optimal for linear systems with Gaussian noise. The example is to track a vehicle running at a constant but unknown speed and subject to random noise [4]. The motion dynamics of the vehicle is given as follows:

$$\begin{bmatrix} x_{1,k+1} \\ x_{2,k+1} \end{bmatrix} = \begin{bmatrix} 1 & 1 \\ 0 & 1 \end{bmatrix} \begin{bmatrix} x_{1,k} \\ x_{2,k} \end{bmatrix} + \begin{bmatrix} 0 \\ 1 \end{bmatrix} w_k \quad (37)$$

and the measurement model is given as follows:

$$y_k = [1 \quad 0] x_k + v_k \quad (38)$$

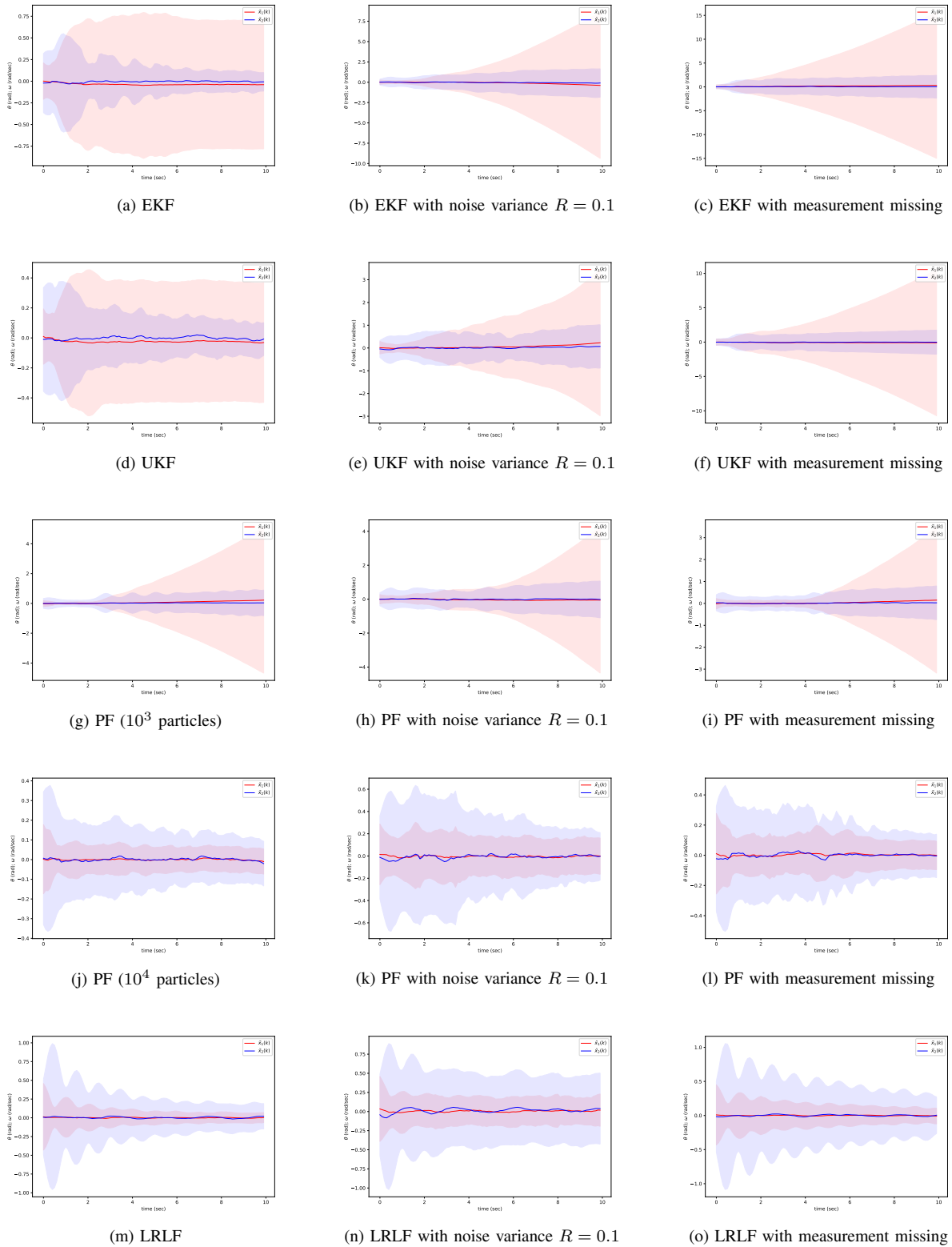


Fig. 5: State estimate error of different methods under different conditions. The left column corresponds to those with simulation setup with the measurement noise variance $R = 0.01$; the middle column corresponds to those with the increased measurement noise variance $R = 0.1$; the right column corresponds to those with measurement missing happening with the probability 0.5. Solid line indicates the average estimate error $\tilde{x}_{1,k}$ (red) and $\tilde{x}_{2,k}$ (blue) and shadowed region for the 1-SD confidence interval. All results are obtained from 500 Monte Carlo runs.

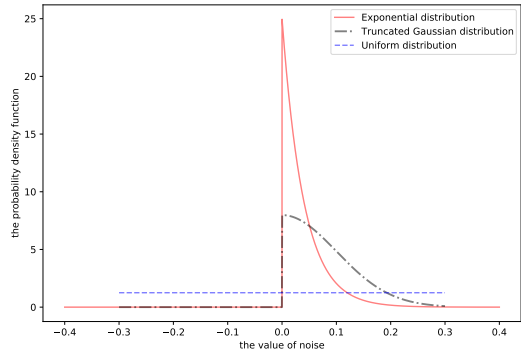


Fig. 6: The PDFs of the three kinds of non-Gaussian noise, e.g., the truncated Gaussian, the exponential and the uniform distributions that we tested with the LRLF.

where $x_{1,k}$, $x_{2,k}$ are the distance and speed of the vehicle at time instant k , respectively. The Gaussian noise $w_k \sim \mathcal{N}(0, 0.01)$ and $v_k \sim \mathcal{N}(0, 0.02)$, and the initial state and the initial state estimate are $x_0 = \begin{bmatrix} 0 \\ 10 \end{bmatrix}$, $\hat{x}_0 \sim \mathcal{N}\left(\begin{bmatrix} 0 \\ 10 \end{bmatrix}, \begin{bmatrix} 0.02 & 0 \\ 0 & 0.03 \end{bmatrix}\right)$, respectively.

We use the same experimental setup as in the previous example of tracking pendulum. The estimate error of the LRLF is obtained from 500 Monte Carlo simulations, as shown in Fig. 8. The SD of state estimate error of the Kalman filter is plotted in Fig. 8 for comparison. It can be found that our proposed LRLF estimate both the distance and speed of the vehicle quite accurately, with slightly bigger estimate error than that of the optimal Kalman filter, which is expected since no state estimators can perform better than the optimal Kalman filter for linear stochastic systems with Gaussian noise.

E. Airborne target tracking case study

We consider the scenario presented in [47], where an unmanned aerial vehicle equipped with a gimballed camera to track a ground vehicle manoeuvring on a road section. Assume that the bearing-only camera platform is kept at the altitude $z^s = 100m$ above the origin of the local coordinate and the road is flat. The camera provides the azimuth angle (ζ) and elevation angle (η) to the target with respect to the camera platform, as described by the following observation model:

$$z_k = h(x_k) = \begin{bmatrix} \zeta_k \\ \eta_k \end{bmatrix} = \begin{bmatrix} \arctan_2(y_k, x_k) \\ \arctan_2(z^s, \sqrt{x_k^2 + y_k^2}) \end{bmatrix} + v_k \quad (39)$$

where $x_k = [s_k^x, s_k^y, \dot{s}_k^x, \dot{s}_k^y]^T$ is the target vehicle's state of position and speed components in x and y direction. The sensor noise v_k is zero-mean Gaussian noise with the covariance $R = \begin{bmatrix} 8 & 0 \\ 0 & 0.002 \end{bmatrix}$.

The target vehicle dynamics is described by a white noise acceleration motion model [48]:

$$x_{k+1} = \begin{bmatrix} 1 & 0 & T & 0 \\ 0 & 1 & 0 & T \\ 0 & 0 & 1 & 0 \\ 0 & 0 & 0 & 1 \end{bmatrix} x_k + \begin{bmatrix} 0.5T^2 & 0 \\ 0 & 0.5T^2 \\ T & 0 \\ 0 & T \end{bmatrix} w_k \quad (40)$$

where the sampling time $T = 0.1s$ and the process noise is zero-mean Gaussian noise with the covariance $Q = \begin{bmatrix} 1 & 0 \\ 0 & 1 \end{bmatrix}$, the initial state and the initial state estimate are $x_0 = \begin{bmatrix} 98 \\ 0 \\ 0 \\ 10 \end{bmatrix}$, $\hat{x}_0 \sim \mathcal{N}\left(\begin{bmatrix} 98 \\ 0 \\ 0 \\ 10 \end{bmatrix}, \begin{bmatrix} 25 & 0 & 0 & 0 \\ 0 & 25 & 0 & 0 \\ 0 & 0 & 1 & 0 \\ 0 & 0 & 0 & 1 \end{bmatrix}\right)$, respectively.

We use the same experimental setup as in the previous example on tracking pendulum. The state estimate of the LRLF obtained from 500 Monte Carlo simulations is shown in Fig. 9. It shows that the proposed LRLF can track the target vehicle's state quite well.

VI. CONCLUSION AND DISCUSSION

This paper has combined Lyapunov's method in control theory and deep reinforcement learning to design state estimator for discrete-time nonlinear stochastic systems. We theoretically prove the convergence of bounded estimate error solely using the data in a model-free manner. In our approach, the filter gain is approximated by a deep neural network and trained offline. During inference, the learned filter can be deployed efficiently without extensive online computations. Simulation results show the superiority of our state estimator design method over existing nonlinear filters, in terms of estimate convergence even under some system uncertainties such as covariance shift in system noise and randomly missing measurements. As initial research developing the RL approach for state estimation, there are still quite a few issues that have not yet addressed in the work. For example, How to quantify uncertainty of the state estimate, i.e., the covariance of state estimate error? What is the convergence bound of state estimate error with finite samples? They will be left as our future research directions.

REFERENCES

- [1] B. D. Anderson and J. B. Moore, *Optimal filtering*. Courier Corporation, 2012.
- [2] S. Thrun, W. Burgard, and D. Fox, *Probabilistic robotics*. MIT press Cambridge, 2005.
- [3] Y. Bar-Shalom, X. R. Li, and T. Kirubarajan, *Estimation with applications to tracking and navigation: theory algorithms and software*. John Wiley & Sons, 2004.
- [4] S. Särkkä, *Bayesian filtering and smoothing*. Cambridge University Press, 2013.
- [5] R. E. Kalman, "A new approach to linear filtering and prediction problems," *Transactions of the ASME – Journal of Basic Engineering*, vol. 82, pp. 35–45, 1960.
- [6] S. J. Julier and J. K. Uhlmann, "Unscented filtering and nonlinear estimation," *Proceedings of the IEEE*, vol. 92, no. 3, pp. 401–422, 2004.
- [7] A. Doucet, S. Godsill, and C. Andrieu, "On sequential monte carlo sampling methods for bayesian filtering," *Statistics and Computing*, vol. 10, no. 3, pp. 197–208, 2000.
- [8] M. Boutayeb, H. Rafaralahy, and M. Darouach, "Convergence analysis of the extended kalman filter used as an observer for nonlinear deterministic discrete-time systems," *IEEE Transactions on Automatic Control*, vol. 42, no. 4, pp. 581–586, 1997.
- [9] K. Reif, S. Gunther, E. Yaz, and R. Unbehauen, "Stochastic stability of the discrete-time extended kalman filter," *IEEE Transactions on Automatic Control*, vol. 44, no. 4, pp. 714–728, 1999.
- [10] L. Li and Y. Xia, "Stochastic stability of the unscented kalman filter with intermittent observations," *Automatica*, vol. 48, no. 5, pp. 978–981, 2012.

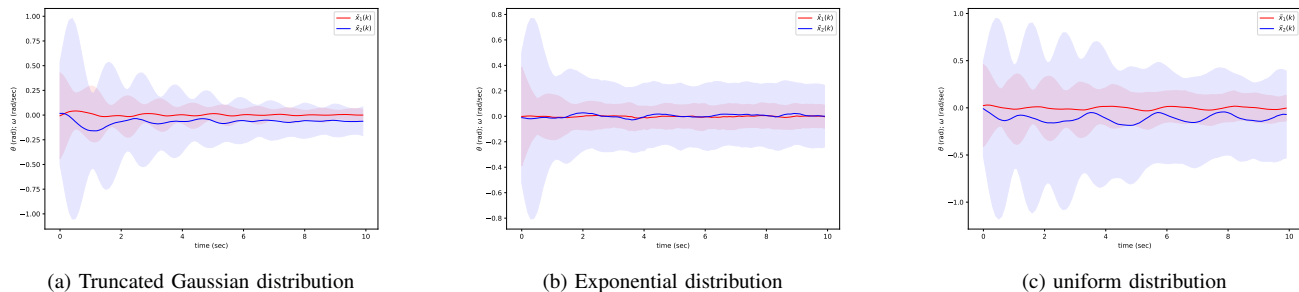


Fig. 7: State estimate error of the LRLF with different kinds of measurement noise shown in Fig. 6. Solid line indicates the average estimate error $\tilde{x}_{1,k}$ (red) and $\tilde{x}_{2,k}$ (blue) and shadowed region for the 1-SD confidence interval. The results are obtained from 500 Monte Carlo runs.

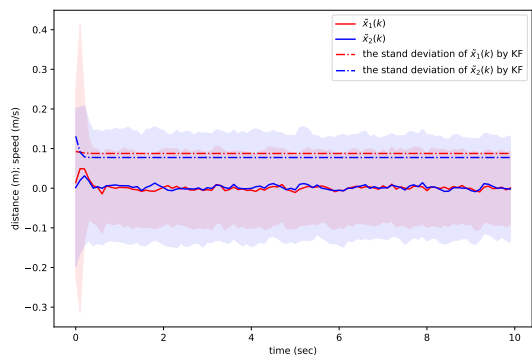


Fig. 8: State estimate error of the LRLF vs the SD of state estimate of the Kalman filter. Solid line indicates the average estimate error $\tilde{x}_{1,k}$ (red) and $\tilde{x}_{2,k}$ (blue) and shadowed region for the 1-SD confidence interval of the LRLF. The results of LRLF are obtained with 500 Monte Carlo runs.

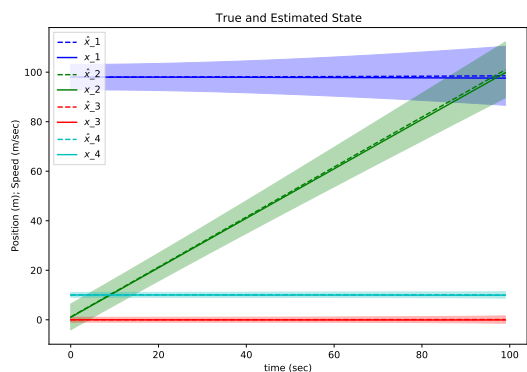


Fig. 9: The true state of target vehicle and state estimate using the LRLF. Solid lines indicate true state and dashed lines the state estimate and shadowed region for the 1-SD confidence interval of the LRLF. The results of LRLF are obtained with 500 Monte Carlo runs.

- [11] D. Crisan and A. Doucet, "A survey of convergence results on particle filtering methods for practitioners," *IEEE Transactions on Signal Processing*, vol. 50, no. 3, pp. 736–746, 2002.
- [12] J. Morimoto and K. Doya, "Reinforcement learning state estimator," *Neural Computation*, vol. 19, no. 3, pp. 730–756, 2007.
- [13] L. Buşoniu, T. de Bruin, D. Tolić, J. Kober, and I. Palunko, "Reinforcement learning for control: Performance, stability, and deep approximators," *Annual Reviews in Control*, 2018.
- [14] A. Tsiamis, N. Matni, and G. J. Pappas, "Sample complexity of kalman filtering for unknown systems," *arXiv preprint arXiv:1912.12309*, 2019.
- [15] N. Yadaiah and G. Sowmya, "Neural network based state estimation of dynamical systems," in *The 2006 IEEE International Joint Conference on Neural Network Proceedings*. IEEE, 2006, pp. 1042–1049.
- [16] R. Wilson and L. Finkel, "A neural implementation of the kalman filter," *Advances in neural information processing systems*, vol. 22, pp. 2062–2070, 2009.
- [17] R. G. Krishnan, U. Shalit, and D. Sontag, "Deep kalman filters," *arXiv preprint arXiv:1511.05121*, 2015.
- [18] D. Gorges, "Relations between model predictive control and reinforcement learning," *IFAC-PapersOnLine*, vol. 50, no. 1, pp. 4920–4928, 2017.
- [19] R. Postoyan, L. Buşoniu, D. Nešić, and J. Daafouz, "Stability analysis of discrete-time infinite-horizon optimal control with discounted cost," *IEEE Transactions on Automatic Control*, vol. 62, no. 6, pp. 2736–2749, 2017.
- [20] J. J. Murray, C. J. Cox, and R. E. Saeks, "The adaptive dynamic programming theorem," in *Stability and control of dynamical systems with applications*. Springer, 2003, pp. 379–394.
- [21] M. Abu-Khalaf and F. L. Lewis, "Nearly optimal control laws for nonlinear systems with saturating actuators using a neural network hjb approach," *Automatica*, vol. 41, no. 5, pp. 779–791, 2005.
- [22] Y. Jiang and Z.-P. Jiang, "Global adaptive dynamic programming for continuous-time nonlinear systems," *IEEE Transactions on Automatic Control*, vol. 60, no. 11, pp. 2917–2929, 2015.
- [23] D. V. Prokhorov, "A Lyapunov machine for stability analysis of nonlinear systems," in *Proceedings of 1994 IEEE International Conference on Neural Networks (ICNN'94)*, vol. 2. IEEE, 1994, pp. 1028–1031.
- [24] D. V. Prokhorov and L. A. Feldkamp, "Application of svm to Lyapunov function approximation," in *IJCNN'99. International Joint Conference on Neural Networks. Proceedings (Cat. No. 99CH36339)*, vol. 1. IEEE, 1999, pp. 383–387.
- [25] T. J. Perkins and A. G. Barto, "Lyapunov design for safe reinforcement learning," *Journal of Machine Learning Research*, vol. 3, no. Dec, pp. 803–832, 2002.
- [26] V. Petridis and S. Petridis, "Construction of neural network based lyapunov functions," in *The 2006 IEEE International Joint Conference on Neural Network Proceedings*. IEEE, 2006, pp. 5059–5065.
- [27] S. M. Richards, F. Berkenkamp, and A. Krause, "The Lyapunov neural network: Adaptive stability certification for safe learning of dynamical systems," in *Conference on Robot Learning*, 2018, pp. 466–476.
- [28] F. Berkenkamp, M. Turchetta, A. Schoellig, and A. Krause, "Safe model-based reinforcement learning with stability guarantees," in *Advances in Neural Information Processing Systems*, 2017, pp. 908–918.
- [29] M. Han, L. Zhang, J. Wang, and W. Pan, "Actor-critic reinforcement learning for control with stability guarantee," *arXiv preprint arXiv:2004.14288*, 2020.

- [30] Q. Zhang, W. Pan, and V. Reppa, "Model-reference reinforcement learning control of autonomous surface vehicles with uncertainties," *arXiv preprint arXiv:2003.13839*, 2020.
- [31] —, "Model-reference reinforcement learning for collision-free tracking control of autonomous surface vehicles," *arXiv preprint arXiv:2008.07240*, 2020.
- [32] R. S. Sutton and A. G. Barto, *Reinforcement learning: An introduction*. MIT press, 2018.
- [33] T. Haarnoja, A. Zhou, P. Abbeel, and S. Levine, "Soft actor-critic: Off-policy maximum entropy deep reinforcement learning with a stochastic actor," in *Proceedings of the 35th International Conference on Machine Learning (ICML 2018)*, vol. 80, Stockholm, Sweden, Jul. 2018, pp. 1861–1870.
- [34] A. M. Lyapunov, *The general problem of the stability of motion (in Russian)*. PhD Dissertation, Univ. Kharkov, 1892.
- [35] Y. Jiang and Z.-P. Jiang, "Computational adaptive optimal control for continuous-time linear systems with completely unknown dynamics," *Automatica*, vol. 48, no. 10, pp. 2699–2704, 2012.
- [36] F. L. Lewis, D. Vrabie, and V. L. Syrmos, *Optimal control*. John Wiley & Sons, 2012.
- [37] C. C. Moore, "Ergodic theorem, ergodic theory, and statistical mechanics," *Proceedings of the National Academy of Sciences*, vol. 112, no. 7, pp. 1907–1911, 2015.
- [38] O. Peters, "The ergodicity problem in economics," *Nature Physics*, vol. 15, no. 12, pp. 1216–1221, 2019.
- [39] R. S. Sutton, H. R. Maei, and C. Szepesvári, "A convergent $o(n)$ temporal-difference algorithm for off-policy learning with linear function approximation," in *Advances in neural information processing systems*, 2009, pp. 1609–1616.
- [40] J. Bhandari, D. Russo, and R. Singal, "A finite time analysis of temporal difference learning with linear function approximation," *arXiv preprint arXiv:1806.02450*, 2018.
- [41] S. P. Meyn and R. L. Tweedie, *Markov chains and stochastic stability*. Springer Science & Business Media, 2012.
- [42] H. L. Royden, *Real analysis*. Krishna Prakashan Media, 1968.
- [43] G. E. Dahl, T. N. Sainath, and G. E. Hinton, "Improving deep neural networks for lvcsr using rectified linear units and dropout," in *Proceedings of 2013 IEEE International Conference on Acoustics, Speech and Signal Processing*, Vancouver, BC, Canada, May 2013.
- [44] M. P. Deisenroth, R. D. Turner, M. F. Huber, U. D. Hanebeck, and C. E. Rasmussen, "Robust filtering and smoothing with gaussian processes," *IEEE Transactions on Automatic Control*, vol. 57, no. 7, pp. 1865–1871, 2011.
- [45] B. Sinopoli, L. Schenato, M. Franceschetti, K. Poolla, M. I. Jordan, and S. S. Sastry, "Kalman filtering with intermittent observations," *IEEE Transactions on Automatic Control*, vol. 49, no. 9, pp. 1453–1464, 2004.
- [46] Z. Wang, B. Shen, and X. Liu, " H_∞ filtering with randomly occurring sensor saturations and missing measurements," *Automatica*, vol. 48, no. 3, pp. 556–562, 2012.
- [47] C. Liu, B. Li, and W.-H. Chen, "Particle filtering with soft state constraints for target tracking," *IEEE Transactions on Aerospace and Electronic Systems*, vol. 55, no. 6, pp. 3492–3504, 2019.
- [48] X. R. Li and V. P. Jilkov, "Survey of maneuvering target tracking. part i. dynamic models," *IEEE Transactions on aerospace and electronic systems*, vol. 39, no. 4, pp. 1333–1364, 2003.